Broadband effective magnetic response of inorganic dielectric resonator-based metamaterial for microwave applications

Riad Yahiaoui, U-Chan Chung, Shah Nawaz Burokur, A. De Lustrac, Catherine Elissalde, Mario Maglione, Valerie Vigneras, Patrick Mounaix

Broadband effective magnetic response of inorganic dielectric resonator-based metamaterial for microwave applications

R. Yahiaoui · U.-C. Chung · S.N. Burokur · A. de Lustrac · C. Elissalde · M. Maglione · V. Vigneras · P. Mounaix

Abstract A single-sized dielectric cylinder-based metama-terial is fabricated from TiO_2 nanoparticles, using a bottom-up approach. The sub-elements constituting the metalayer are embedded in a nonmagnetic transparent host matrix in the microwave regime and arranged in a square lattice. We demonstrate numerically and experimentally a broad-band magnetic activity. The key feature to achieve this per-formance remains in the high aspect ratio of the metama-terial building blocks. This is a very promising step to-wards complex electromagnetic functions, involving low-cost metamaterials with simple fabrication.

1 Introduction

Metamaterials with their unusual properties constitute a very promising research topic. They are increasingly used to build various electromagnetic functions, such as radiation, filtering, absorption, coupling, amplification, and super-resolution. Usually based on metallic patterns printed on dielectric substrates, metamaterials have undergone considerable growth and development since the pioneering work of V.G. Veselago [1], related to negative index materials (NIMs). These latter materials remained for a long time as a "scientific fiction" due to the unavailability of such mate-rials in nature. NIMs have been made possible thanks to J.B. Pendry et al., with their composite structure, which combines plasmonic wires (PWs) [2] and split ring res-onators (SRRs) [3] and subsequently paved the way to a first experimental demonstration by R.A. Shelby et al. [4]. The major drawbacks of using metallic inclusions are their anisotropy, significant conduction losses near the resonant frequencies, and manufacturing difficulties at higher frequencies. Furthermore, they inherently suffer from very narrow bandwidth resonant modes, thus limiting their electromagnetic performance. Recently, a novel class of metamaterials involving high-permittivity dielectric particles has been introduced and has been the subject of intense research ac-tivity [5–10]. These so-called all-dielectric metamaterials, whose operating principle is based on the Mie theory, offer possibilities to achieve isotropic and low-loss metamaterials. They have been explored for their potential use in dielectric resonator antennas (DRAs) [11], magnetic resonance imaging (MRI) [12], cloaking [13, 14], and electromagnetically induced transparency (EIT) [15]. Once exposed to an exciting electromagnetic plane wave and due to the high-permittivity materials used, a series of Mie modes are developed within the particles, which are accompanied by resonances on the magnetic and/or electric spectra. Moreover,

R. Yahiaoui (✉)
XLIM, Univ. Limoges, CNRS, UMR 6172, 7 rue Jules Vallès, 19100 Brive, France
e-mail: riad.yahiaoui@unilim.fr

U.-C. Chung · C. Elissalde · M. Maglione
ICMCB, Univ. Bordeaux, CNRS, UPR 9048, 87 avenue du Docteur Albert Schweitzer, 33600 Pessac Cedex, France

V. Vigneras
IMS, Univ. Bordeaux, CNRS, UMR 5218, 16 avenue Pey Berland, 33600 Pessac Cedex, France

S.N. Burokur · A. de Lustrac
IEF, Univ. Paris-Sud, CNRS, UMR 8622, 91405 Orsay Cedex, France

S.N. Burokur · A. de Lustrac
Univ. Paris-Ouest, 92410 Ville d'Avray, France

P. Mounaix
LOMA, Univ. Bordeaux, CNRS, UMR 5798, 351 Cours de la Libération, 33405 Talence Cedex, France

by using sets of dielectric spheres with two different sizes embedded in a dielectric matrix, Vendik et al. demonstrated analytically and numerically a double negative (DNG) behavior at microwave frequencies. The negative refractive index is expected in the frequency region where TM-mode resonance in one of the two sets of particles and TE-mode resonance in the other occur simultaneously [16]. Later on, other authors used the same concept and proposed negative refractive index media involving a TiO_2 cube array and a BST/Mn rod array, respectively [16, 17]. More recently, Lai et al. suggested a hybrid structure based on two kinds of dielectric resonators, namely ZrO_2 cuboids and Al_2O_3 cubes to achieve a low-loss and high-symmetry NIM in the microwave regime [18]. In this study, single-sized dielectric-resonator-based metamaterial exhibiting a broadband magnetic activity is demonstrated numerically and through experimental measurements at microwave frequencies, in the 5–10 GHz frequency band.

2 The investigated periodic medium

Let us first consider a periodic array of titanium dioxide (TiO_2) cylinder resonators (depicted in the inset of Fig. 1a with relative dielectric permittivity $\varepsilon_r \sim 90$, loss tangent $\tan\delta \sim 0.05$, diameter $d = 0.5$ cm, thickness $t = 2.8$ mm, and periodicity $p = 1$ cm) organized in a square lattice. The dielectric-resonator-based metamaterial is excited by an electromagnetic plane wave at normal incidence, with a specific polarization of the electric and magnetic fields, as depicted in the left panel of Fig. 1b. Note that one single metalayer is taken into account along the direction of propagation k. Using the finite element method based full-wave electromagnetic simulator HFSS®, numerical simulations are performed to predict the spectral response of the structure. The transmission spectrum is depicted in Fig. 1a and reveals a series of Mie modes around 7.5 GHz, 8.9 GHz, and 12.3 GHz approximately (denoted by arrows in Fig. 1a). This resonant behavior is closely connected to the high value of the relative permittivity of TiO_2. Indeed, high values of permittivity are necessary to support Mie resonances within the particles and to ensure that their dimensions are considerably less than the wavelength in the host medium in order to avoid the diffraction effect [16].

Using the standard retrieval method [19], the effective permittivity and permeability are extracted from the complex transmittance and reflectance spectra and are shown in Fig. 1a. One can observe that the aforementioned Mie modes are accompanied by a series of electric and magnetic resonances. Indeed, the first Mie mode occurring at about 7.5 GHz results in a resonant effective permeability, and the TiO_2 cylinder behaves as a magnetic dipole. An antiresonant behavior of the permittivity associated with a negative

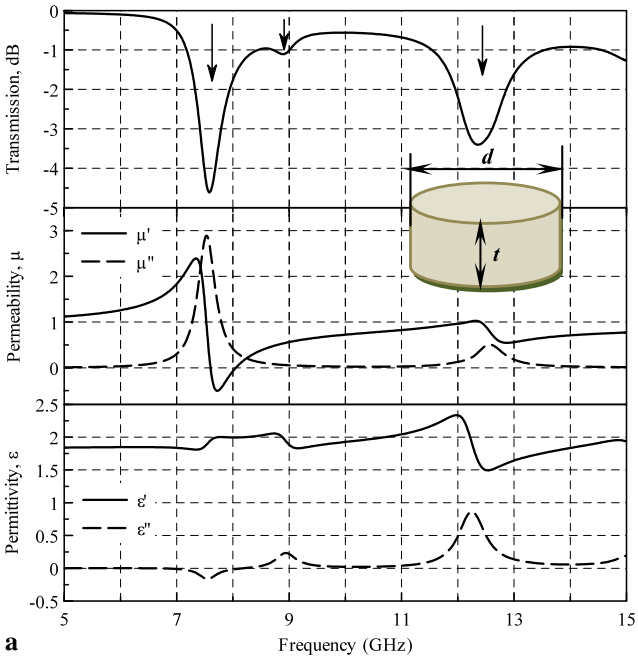

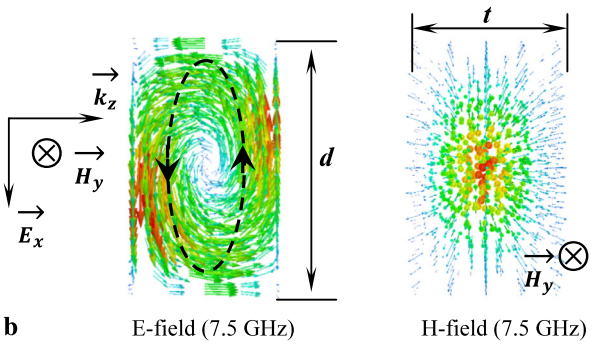

Fig. 1 (**a**) Calculated amplitude transmittance of the TiO_2-cylinder-based metamaterial ($d = 0.5$ cm, $t = 2.8$ mm), extracted effective permeability μ, and effective permittivity ε, respectively. The unit cell of our investigated metamaterial is represented in the inset of Fig. 1a. (**b**) Electric and magnetic field distributions inside the TiO_2 cylinder for the first-order magnetic mode (around 7.5 GHz). *Black dashed line* and *arrows* indicate the direction of the electric field, while the *incoming cross* shows the magnetic field direction. The polarization of the incident electromagnetic plane wave is also depicted in the figure

imaginary part appears at the same frequency, which is inherent to periodic structures, as pointed out by some authors [20, 21].

The second-lowest mode, located at about 8.9 GHz, exhibits a resonant electric permittivity and is similar to an electric dipole. The third Mie mode, which occurs at about 12.3 GHz, results simultaneously in a resonant magnetic permeability and electric permittivity. The spatial distribution of electric and magnetic fields around the first Mie mode within a unit cell of our metamaterial is plotted in Fig. 1b. Basically, the wave front of an incident electromagnetic plane wave undergoes a strong distortion close to the metamaterial in order to satisfy simultaneously the con-

tinuity and discontinuity conditions of tangential and normal electric field components at the cylinder-air interfaces, respectively. The electric field, developed inside the TiO_2 cylinder, is then predominantly tangential close to its surface. This leads to the creation of displacive eddy currents in the cylinder cross section, which enhance the magnetic field confined along the y axis (denoted by an incoming cross in the right panel of Fig. 1b). A resonant behavior is then expected at this specific frequency [7], and the cylinders are then viewed as the counterparts of the potential wells, which confine electrons in quantum systems. Considered as the degree of magnetization that a material obtains in response to an applied magnetic field, the effective magnetic permeability of our investigated metamaterial follows a typical Lorentz-like model according to the following expression:

$$\mu(\omega) = 1 - \frac{A\omega^2}{\omega^2 - \omega_{mp}^2 - j\Gamma\omega} \tag{1}$$

where A is a constant, ω_{mp} is the magnetic plasma frequency, and Γ is the damping factor, representing losses and scattering mechanisms. The effective magnetic permeability shows a resonant behavior, which leads to negative values of μ within a frequency band between the resonant frequency ω_0 and the magnetic plasma frequency ω_{mp} (see Fig. 1a). Below the magnetic resonant frequency, the real part of the permeability tends to unity $\mathrm{Re}(\mu) = 1$. Beyond the resonant magnetic frequency, the incident electromagnetic field is shielded by metallic patterns, the inclusions exhibit a diamagnetic behavior, μ is negative, and the generated magnetic induction $B = \mu H$ is opposite to the incident magnetic field H. At high frequencies, the permeability μ lies between 0 and 1. The region of the magnetic function located below the resonant frequency is very promising for low-loss applications, such as inductor cores, transformer cores, and magnetic recording heads. The zone of the permeability around the resonant frequency is more appropriate for high-loss applications, like filtering, and high-frequency parasitic absorber applications.

3 Broadband magnetic activity achievement

The bandwidth of a metamaterial is an important criterion that may be very valuable in various applications, such as band-pass filters, wavelength division multiplexers, and antenna systems. Due to the resonant nature of metamaterials, their electromagnetic properties are restricted to very narrow frequency bands, thus limiting their functioning. However, multiple-band metamaterials with specific narrow frequencies have already been demonstrated in the scientific literature [22, 23]. They are considered as a starting point to reach broadband metamaterials [24–26]. In this section, we propose a very unique approach to achieve a symmetric metamaterial with broadband magnetic activity (negative permeability). Indeed, a much broader continuous band of negative effective permeability μ' can be achieved by taking advantage of the large aspect ratio of the unit cell constituting the metamaterial ($d \gg t$).

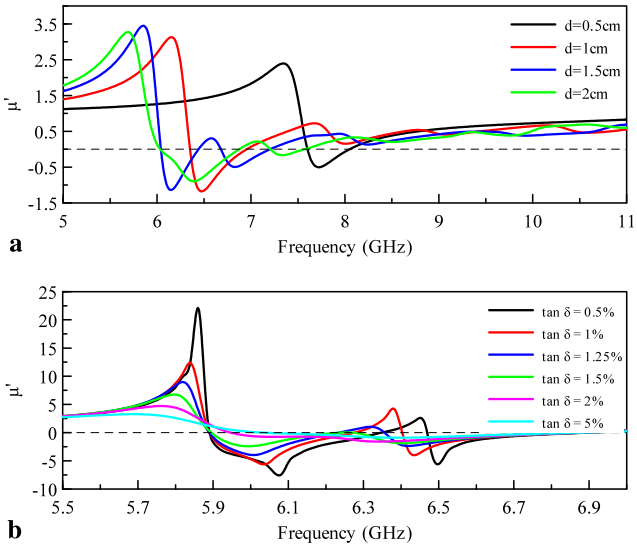

Fig. 2 (**a**) Calculated real parts of the magnetic permeability μ' for several diameters d of TiO_2 cylinders varying from 0.5 cm to 2 cm ($t = 2.8$ mm, $\varepsilon_r \sim 90$, $\tan\delta \sim 5$ %). (**b**) Real parts of the effective permeability μ' for $d = 2$ cm, and $\tan(\delta)$ varying from 0.5 % to 5 %

Here we consider a metalayer made of a single type of cylinder with diameter d varying from 0.5 cm to 2 cm, while the thickness of the cylinders $t = 2.8$ mm is kept constant. Note that the period p of the lattice has been fixed to $d + 0.5$ cm each time, and the dielectric properties of TiO_2 are $\varepsilon_r \sim 90$, and $\tan\delta \sim 5$ %. The numerical effective parameters retrieved by the inversion of Fresnel equations [19] for different values of the diameter d of the disks are given in Fig. 2a. The permeability is highly dispersive and exhibits a spectral region of Lorentz-like behavior in accordance with Mie theory. For diameter $d \geq 2$ mm, the position of the first Mie resonance does not shift significantly and it is mainly imposed by the thickness t of the disks. By contrast, upon increasing d, the distance between the first and higher order modes decreases, and by making sure that $d \gg t$, the resonances can overlap, thus giving rise to a much broader continuous frequency region of negative μ' (Fig. 2a), resulting from mutual coupling between spectrally adjacent resonances. For example, the retrieved effective μ' for $d = 0.5$ cm is negative within 7.58 GHz–8 GHz, but for higher cylinder diameters, this range is much broader; for $d = 2$ cm it spreads from 6 GHz to about 6.8 GHz.

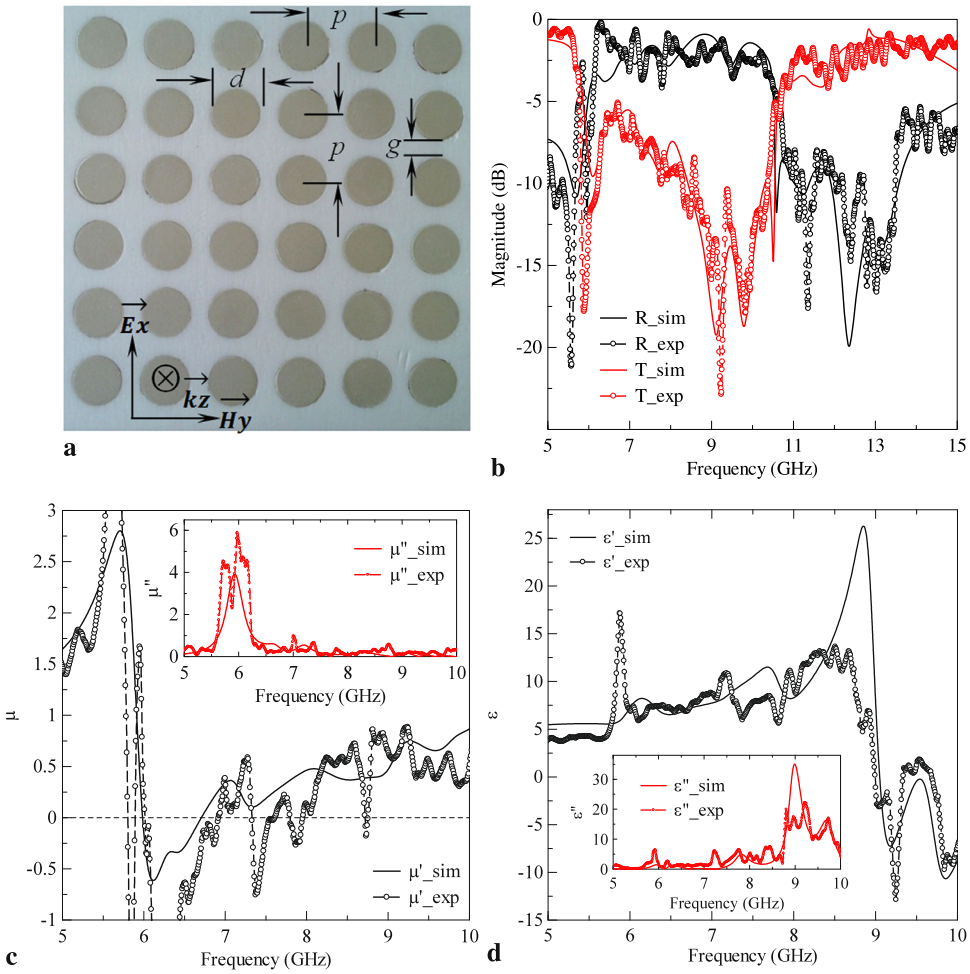

Fig. 3 (**a**) The dielectric resonator-based metamaterial ($d = 2$ cm, $p = 2.8$ cm, $g = 0.8$ cm, and $t = 2.8$ mm) embedded in a 3 mm thick Rohacell® foam matrix. (**b**) Simulated (*solid lines*) and measured (*lines and symbols*) magnitudes of the transmission and reflection spectra. (**c**) Real and imaginary parts of the effective permeability. (**d**) Real and imaginary parts of the effective permittivity

The presence of losses is an inevitable consequence of the underlying resonances. It may seem paradoxical, but it turns out that dielectric losses contribute favorably to obtain a broad spectral region of negative μ'. We have already demonstrated this apparently counter-intuitive effect using a $SrTiO_3$ rod-based metamaterial in the terahertz regime [6]. Indeed, we examined the influence of the loss tangent ($\tan\delta$) on the spectrum of the magnetic permeability μ'. Figure 2b shows the effective μ' for $d = 2$ cm and values of tan (δ) from 0.5 % to 5 %. One can observe that μ' is negative over a broad frequency range only if the dielectric losses reach a sufficiently high level. We propose an optimum loss tangent of 2 %, leading to a large bandwidth of negative μ' extending from 5.94 GHz to 6.8 GHz. Upon the increase of tan(δ), the resonances become smoother and their magnitude decreases. In short, a large frequency band of negative μ' is achieved at the expense of low amplitude. Metamaterial-based applications do not necessarily need large values of μ', particularly in the field of sub-wavelength focusing, where $\mu' = -1$ is highly desired, since it constitutes one of the required conditions to achieve a perfect-lens effect [27].

4 Experimental characterizations

To confirm the numerical predictions, we have fabricated an experimental prototype using a bottom-up approach. The starting material was commercial titanium dioxide (TiO_2) powder, which was pressed into pellets and then sintered in a tube furnace at 1300 °C for 4 hours under an oxygen-enriched atmosphere to reach well-densified (∼98 %) cylinders with diameter $d = 2$ cm and a thickness $t = 2.8$ mm. 48 dielectric resonators have been fabricated and then embedded in a 22.4 cm × 16.8 cm commercial nonmagnetic host Rohacell® foam matrix ($\varepsilon_h \sim 1.02$, $\tan\delta_h = 0.002$) to form a periodic array with an optimal periodicity $p = 2.8$ cm along the Ex and Hy directions, corresponding to a filling factor of about 40 % when $d = 2$ cm. Although the diameter d and the periodicity p of the unit cell of the proposed metamaterial along the x and y directions are not much smaller than the guided wavelength, diffraction still cannot occur. The reason is that the electromagnetic waves are not propagating along the x and y directions (see Fig. 3a). A similar effect was observed in the so-called fishnet-metamaterial [28], proposed as an alternative to the conventional struc-

ture, which combines split ring resonators (SRRs) and continuous wires (CWs) to achieve a negative refractive index. On the other side, we will find that the thickness t of the elementary cell along the z direction is much smaller than the electromagnetic resonance wavelength (about $\lambda/18$). Thus, the effective medium model is successfully applied. We consider here the case of a single metalayer along the direction of propagation k, illuminated by a plane wave at normal incidence, with an appropriate polarization of the electric and magnetic field, as depicted in Fig. 3a. Microwave measurements based on the experimental setup described in [29] have been done on a fabricated prototype in an anechoic chamber using an Agilent 8722ES vector network analyzer and two 2–18 GHz wideband horn antennas. Phase referencing and normalization have been performed in transmission by removing the sample from the signal path, and in reflection, by replacing the sample with a copper plate. The magnitudes of transmission and reflection coefficients are plotted in Fig. 3b for the 5–15 GHz frequency band. A good quantitative agreement between simulation and experiment is obtained. One can observe a band-gap behavior having a -10 dB bandwidth of about 2 GHz from 8.5 GHz to 10.5 GHz approximately in both simulation and experiment.

The effective magnetic permeability μ was retrieved from simulated and measured data and plotted in Fig. 3c. The effective electric permittivity is depicted in Fig. 3d. It exhibits a resonant behavior around 9 GHz, and reaches negative values over a broad frequency range. Although there are minor differences in amplitude and bandwidth due to manufacturing imperfections, the effective magnetic permeability and effective electric permittivity retrieved from measurements confirm very well the trend obtained from simulations. Note that an infinite structure was considered in simulations, while a prototype with realistic dimensions (22.4×16.8 cm^2) was characterized experimentally, thus favoring the discrepancies between simulation and experiment.

5 Conclusions

In summary, we successfully fabricated a single-sized dielectric-resonator-based metamaterial out of TiO_2 nanoparticles exhibiting a broadband magnetic activity. By taking advantage of the large size ratio of the unit cell of the metamaterial (i.e., $d \gg t$), we have proposed a very unique approach for achieving a broad spectral region of negative effective permeability in accordance with Mie theory. The proposed structure is very promising for absorber and filtering applications, where large levels of losses (namely around the magnetic and/or electric resonant frequencies) are highly desired in the frequency band to be rejected.

Acknowledgement This work has been performed in the framework of the project: "GIS-AMA-SAMM". The authors would like to thank M. Eddie Maillard for manufacturing the Rohacell® foam matrix, with the LOMA mechanical facilities.

References

1. V.G. Veselago, The electrodynamics of substances with simultaneously negative values of ε and μ. Sov. Phys. Usp. **10**, 509 (1968)
2. J.B. Pendry, A.J. Holden, W.J. Stewart, I. Youngs, Extremely low frequency plasmons in metallic mesostructures. Phys. Rev. Lett. **76**, 4773 (1996)
3. J.B. Pendry, A.J. Holden, D.J. Robbins, W.J. Stewart, Magnetism from conductors and enhanced nonlinear phenomena. IEEE Trans. Microw. Theory Tech. **47**, 2075 (1999)
4. R.A. Shelby, D.R. Smith, S. Schultz, Experimental verification of a negative index of refraction. Science **292**, 77 (2001)
5. Q. Zhao, L. Kang, B. Du, H. Zhao, Q. Xie, X. Huang, B. Li, J. Zhou, L. Li, Experimental demonstration of isotropic negative permeability in a three-dimensional dielectric composite. Phys. Rev. Lett. **101**, 027402 (2008)
6. R. Yahiaoui, H. Němec, P. Kužel, F. Kadlec, C. Kadlec, P. Mounaix, Broadband dielectric terahertz metamaterials with negative permeability. Opt. Lett. **34**, 3541 (2009)
7. H. Němec, P. Kužel, F. Kadlec, C. Kadlec, R. Yahiaoui, P. Mounaix, Tunable terahertz metamaterials with negative permeability. Phys. Rev. B **79**, 241108 (2009)
8. T. Lepetit, E. Akmansoy, J.-P. Ganne, Experimental measurement of negative index in an all-dielectric metamaterial. Appl. Phys. Lett. **95**, 121101 (2009)
9. H. Němec, C. Kadlec, F. Kadlec, P. Kužel, R. Yahiaoui, U.-C. Chung, C. Elissalde, M. Maglione, P. Mounaix, Resonant magnetic response of TiO_2 microspheres at terahertz frequencies. Appl. Phys. Lett. **100**, 061117 (2012)
10. R. Yahiaoui, H. Němec, C. Kadlec, F. Kadlec, P. Kužel, U.-C. Chung, C. Elissalde, M. Maglione, P. Mounaix, TiO_2 microspheres-based metamaterials exhibiting effective magnetic response in the terahertz regime. Appl. Phys. A **109**, 891 (2012)
11. T. Ueda, N. Michishita, M. Akiyama, T. Itoh, Dielectric-resonator-based composite right/left-handed transmission lines and their application to leaky wave antenna. IEEE Trans. Microw. Theory Tech. **56**, 2259 (2008)
12. K. Haines, T. Neuberger, M. Lanagan, E. Semouchkina, A.G. Webb, High Q calcium titanate cylindrical dielectric resonators for magnetic resonance microimaging. J. Magn. Reson. **200**, 349 (2009)
13. D.P. Gaillot, C. Croënne, D. Lippens, An all-dielectric route for terahertz cloaking. Opt. Express **16**, 3986 (2008)
14. E. Semouchkina, D.H. Werner, G.B. Semouchkin, C. Pantano, An infrared invisibility cloak composed of glass. Appl. Phys. Lett. **96**, 233503 (2010)
15. C.K. Chen, Y.C. Lai, Y.H. Yang, C.Y. Chen, T.J. Yen, Inducing transparency with large magnetic response and group indices by hybrid dielectric metamaterials. Opt. Express **20**, 6952 (2012)
16. O.G. Vendik, M.S. Gashinova, Artificial double negative (DNG) media composed by two different dielectric sphere lattices embedded in a dielectric matrix, in *Proc. Eur. Microw. Conf*, (2004), pp. 1209–1212
17. K. Shibuya, K. Takano, N. Matsumoto, K. Izumi, H. Miyazaki, Y. Jimba, M. Hangyo, Terahertz metamaterials composed of TiO_2 cube arrays, in *Proc. Metamaterials Conf*, (2008), pp. 777–779

18. Y.C. Lai, C.K. Chen, Y.H. Yang, T.J. Yen, Low-loss and high-symmetry negative refractive index media by hybrid dielectric resonators. Opt. Express **20**, 2876 (2012)
19. D.R. Smith, S. Schultz, P. Markoš, C.M. Soukoulis, Determination of effective permittivity and permeability of metamaterials from reflection and transmission coefficients. Phys. Rev. B **65**, 195104 (2002)
20. S. O'Brien, J.B. Pendry, Magnetic activity at infrared frequencies in structured metallic photonic crystals. J. Phys. Condens. Matter **14**, 6383 (2002)
21. T. Koschny, P. Markos, D.R. Smith, C.M. Soukoulis, Resonant and antiresonant frequency dependence of the effective parameters of metamaterials. Phys. Rev. E **68**, 065602 (2003)
22. Y. Yuan, C. Bingham, T. Tyler, S. Palit, T.H. Hand, W.J. Padilla, N.M. Jokerst, S.A. Cummer, A dual-resonant terahertz metamaterial based on single-particle electric-field-coupled resonators. Appl. Phys. Lett. **93**, 191110 (2008)
23. H. Li, L.H. Yuan, B. Zhou, X.P. Shen, Q. Cheng, T.J. Cui, Ultra-thin multiband gigahertz metamaterial absorbers. J. Appl. Phys. **110**, 014909 (2011)
24. S. Hrabar, I. Krois, A. Kiricenko, Towards active dispersionless ENZ metamaterial for cloaking applications. Metamaterials **4**, 89 (2010)
25. M. Barbuto, A. Monti, F. Bilotti, A. Toscano, Design of a non-Foster actively loaded SRR and application in metamaterial-inspired components. IEEE Trans. Antennas Propag. **61**, 1219 (2013)
26. K.Z. Rajab, Y. Hao, D. Bao, C.G. Parini, J. Vazquez, M. Philippakis, Stability of active magnetoinductive metamaterials. J. Appl. Phys. **108**, 054904 (2010)
27. J.B. Pendry, Negative refraction makes a perfect lens. Phys. Rev. Lett. **85**, 3966 (2000)
28. C. Yan, Y. Cui, Q. Wang, S. Zhuo, Negative refractive indices of a confined discrete fishnet metamaterial at visible wavelengths. J. Opt. Soc. Am. B **25**, 1815 (2008)
29. J. Zhou, L. Zhang, G. Tuttle, T. Koschny, C.M. Soukoulis, Negative index materials using simple short wire pairs. Phys. Rev. B **73**, 041101(R) (2006)